TECHNICAL PAPER

A new measurement technique for monitoring inorganic scale deposition

Arley Alles Cruz[1,2] · Fabio Cleisto Alda Dossi[1] · Giancarlo Richard Salazar-Banda[2,3] · Elton Franceschi[1,2] · Gustavo Rodrigues Borges[1,2] · Claudio Dariva[1,2]

Abstract

Scale formation is one of the many challenges for flow assurance in the oil and gas industry in deep water oilfields. This work focuses on the development of a new technique for inorganic scale monitoring based on electrical measurements. Experiments were carried out using synthetic water with the composition of a pre-salt Brazilian oilfield. Two different methodologies were applied for fouling formation. The results showed that the multiple-batch methodology increased the content of inorganic deposits on the electrodes, improving the output signal decay analysis of the system. Scanning electron microscopy with energy-dispersive spectroscopy (SEM–EDS) studies was used to validate the presence of fouling deposits, corroborating the sensor's detection efficiency. The spatial distribution of the main scaling chemical elements was also demonstrated by SEM–EDS analysis across the batches. In addition, the effects of temperature and electrode surface orientation were determined. The decay of the sensor output signal increased for higher temperatures (80 °C and 60 °C) compared to 40 °C due to the reduced solubility of $CaCO_3$. For the horizontal position of the electrodes, measurements of the sensor and SEM analysis revealed a greater accumulation of fouling compared to the vertical position.

Keywords Sensor development · Scaling detection · Scales deposition · Flow assurance · Scale prevention

✉ Arley Alles Cruz
arley_alles@hotmail.com

Fabio Cleisto Alda Dossi
fabio_dossi@itp.org.br

Giancarlo Richard Salazar-Banda
gianrsb@gmail.com

Elton Franceschi
elton@itp.org.br

Gustavo Rodrigues Borges
gustavo_rodrigues@itp.org.br

Claudio Dariva
claudio_dariva@itp.org.br

1   Center for Studies on Colloidal Systems (NUESC), Institute of Technology and Research (ITP), Av. Murilo Dantas, 300, Farolândia, Aracaju, SE, Brazil

2   Postgraduate Program in Process Engineering (PEP), Tiradentes University, Av. Murilo Dantas, 300, Farolândia, Aracaju, SE, Brazil

3   Laboratory of Electrochemistry and Nanotechnology (LEN), Institute of Technology and Research (ITP), Av. Murilo Dantas, 300, Farolândia, Aracaju, SE, Brazil

1 Introduction

As global energy consumption continues to increase, fossil fuels remain the primary energy source, putting pressure on the productive sector [1, 2]. The oil and gas industry is expanding its operational domain to deep water to meet the growing demand, which challenges performance and operational integrity. To minimize the downside risk to applications, new technological strategies are required to improve operational system availability, reliability, and maintenance [3].

Scale formation is one of the many challenges for flow assurance in the oil and gas industry in deep water oilfields. The formation, precipitation, and subsequent deposition of mineral-scale particles pose a significant challenge to oilfield facilities due to the risks to personnel safety and system integrity, as well as a substantial financial loss. These solid deposits grow over time, blocking and hindering fluid flow through pipelines at oilfield facilities, causing productivity reduction and unscheduled downtime. Electronic equipment and associated instruments can fail because of adhered solids

and corrosion processes in pipelines, oil and gas separation, pumps, and valves [4, 5].

Inorganic scales are hard crystalline inorganic salt deposits that originate from aqueous solutions when the solute composition exceeds the saturation limit. Despite the variation in the chemical composition of mineral deposits among oilfields, the most common scaling cations come from earthy alkaline: Ca^{2+}, Ba^{2+}, Sr^{2+}, and Mg^{2+} [6]. Most frequently, scaling is produced when formation water mixes with different brines as the injection water. Therefore, both reservoirs and tubular wellbores should be free of scale deposition to assure fluid flow [6, 7].

Operations for treating and preventing inorganic scales demand relevant research and economic efforts [4, 5, 7, 8]. Therefore, monitoring inorganic scale formation is imperative to ensure efficient and economical transport of hydrocarbons through oilfield facilities [9, 10]. For this reason, the development of cutting-edge technologies is relevant for exploring hostile and technologically challenging deepwater fields.

Electrochemical methods are widely used to evaluate the deposition of scales. To determine the optimal cathodic potential for carbonate deposition, linear sweep voltammetry can be used to examine the effects of scale inhibitors (HEDP, PBTCA, PAA) on $CaCO_3$ crystal structure and morphology. In addition to chronoamperometry, electrochemical impedance spectroscopy can be used to monitor $CaCO_3$ deposition and determine the effectiveness of scale inhibition [11]. Nevertheless, there are few studies regarding real-time or near-real-time monitoring of inorganic scale deposition [10]. Some studies relying on the thickness shear-mode resonator (TSMR) technique determine the stability of brine-produced water toward scale formation in oilfield systems [10, 12]. The TSMR method yields accurate results with fast measurement of pipeline scaling, with the potential to be used as a near-real-time monitoring technique. On the other hand, some challenges, such as sensor saturation and loading limit, affect its use in continuous monitoring [13]. Several different strategies have been used to monitor scale deposition under controlled conditions, including the use of minimum inhibitory concentrations to predict $CaCO_3$ scale formation under turbulent flow regimes through filter pores [14], ultrasound measurements coupled with artificial intelligence to monitor petroleum pipelines [15], and radioactive methods (gamma ray systems) to monitor scale detection and thickness [16].

In this scenario, new non-destructive methods for detecting and identifying scale deposits early to optimize hydrocarbon production are needed despite all the current competing technologies. Here, we develop a new technique for monitoring scale deposition based on electrical measurements. Such work will contribute to evaluating some aspects of scale deposition, such as aging, temperature, and substrate surface orientation.

2 Materials and methods

2.1 Measurement principle of the system

For the development of this new fouling measurement technique, electrical measurements were accomplished using a system developed in this study. The primary goal of the developed sensor was to track the difference in electrical conductivity between the solution and the deposited scales. Salts behave as electrical insulators in the solid state (scales) but show conductivity when ionized in aqueous solutions [17]. Then, the conductivity variation can be determined by measuring electrical current based on the Ohm law equation:

$$U = \frac{\rho * l}{A} * I \tag{1}$$

where U is the applied electrical potential, ρ is the electrical conductivity, l is the length of the conductor, A is the conductor transversal area, and I is the electrical current passing through the conductor.

The electrical current amplitude is affected by the conductivity of the sample as a function of the applied electric potential. This sensor applies a potential to the solution by inserting electrodes into a saline solution, which is then monitored using the output current. The output current is influenced by saline solution conductivity (or resistance). In the first moment, the conductivity of the medium is expected to be extremely high because of the large number of ions dissolved in the solution. As scales are formed and tend to deposit on the electrodes, the path of electrical current begins to suffer a decrease in conductivity, reflecting low current values.

2.2 Preparation of synthetic water

This study was based on the influence of water incompatibility on the scale formation process. With that, the developed sensor was evaluated by using a synthetic saline solution. The chemicals used for its preparation were NaCl (99%), $CaCl_2$ (99%), KCl (99%), $MgCl_2$ (99%), $BaCl_2$ (99%), $SrCl_2$ (99%), $NaHCO_3$ (99%), $C_2H_3NaO_2$ (99%), KBr (99%), and Na_2SO_4 (99%). These chemicals were used to produce cationic and anionic waters with the formation of a scaling process due to mixing them. The concentration of ions in the solution must be at a supersaturation level to promote the phenomenon of inorganic formation. For this, the used

Table 1 Ion concentration (ppm) for the brines used to evaluate the behavior of the sensor

Ions	Concentration (ppm)
Cation solution	
Na^+	50,496
Sr^{2+}	252
Ba^{2+}	284
Ca^{2+}	792
Mg^{2+}	305
K^+	391
Cl^-	79,229
Anion solution	
HCO_3^-	1544
SO_4^-	46
$C_2H_3O_2^-$	138

concentration of such components was based on a Brazilian pre-salt oilfield presented in Table 1.

Each chemical was weighed separately using an analytical balance (Shimadzu, model AUX320). The solutes for each brine were mixed and dissolved in ultrapure water to produce 70 ml of each solution. Both solutions were filtered using a vacuum system to remove undissolved salt crystals. After that, the pH of the solutions was adjusted to 7.5 (the same value as oilfield) with NaOH for cation solutions and HCl for anion solutions.

2.3 System operation and components

In summary, the main part of scale measurements consists of the sensor based on electrical measurements. It has a signal generator system, an electric current-to-potential converter, two electrodes made of 316 stainless steel, and a data acquisition system (DAS) (Fig. 1).

The multifunctional instrument Analog Discovery 2 (Digilent) (Fig. 1e) was used to generate sinusoidal input signals with the goal of promoting a proportional sinusoidal output signal (peak-to-peak values) referent of medium resistance. The function waveform generator of Analog Discovery 2 was configured to generate waveforms with amplitude values of 1 V, offset levels of 0 V, and frequencies of 10 kHz. Such frequency was selected in order to reduce the capacitive and inductive impedance effects, and it was found in previous work [18] that evaluated such behavior in high-conductive water systems, as used in this present work. In the same form, the selected amplitude was based on the same report.

An electrode inserted into the reactor sent the input sinusoidal signal (from the signal generator) to the medium (Fig. 1a). A second electrode was introduced into the reactor to complete a circuit in the solution and allow an electrical current to flow. This electrode was linked to an operational amplifier (Texas Instruments, model NE5532), which utilized an inverted amplifier design to convert current to potential. Such a configuration returned an amplified voltage output signal that was proportional to the electrical resistance of the sample, following the equation as follows:

$$U_{out} = -\frac{R_i}{R_x} * U_{in} \tag{2}$$

where U_{out} is the output signal value, R_i is the gain resistor (220 Ohms based on signal adjustment setup), which is responsible for amplifying the signal, R_x is the representation
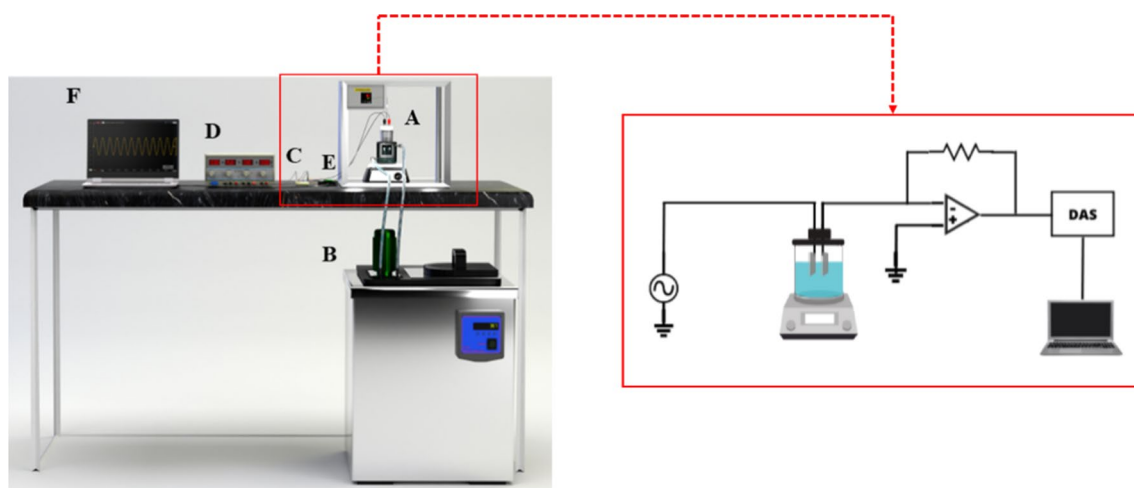

Fig. 1 Schematic of the experimental unit for scale monitoring. The unit is composed of a reactor **A**, a thermostatic batch **B**, a current-to-potential converter circuit **C**, an electrical supply **D**, a multifunctional instrument Analog Discovery 2 **E**, and Visualization system **F**. At the right side, electronic representation of sensor with saline solution in the reactor is shown

Fig. 2 Image of experimental unit used for monitoring scale deposition, with more detail about the reactor and position of electrodes during measurements
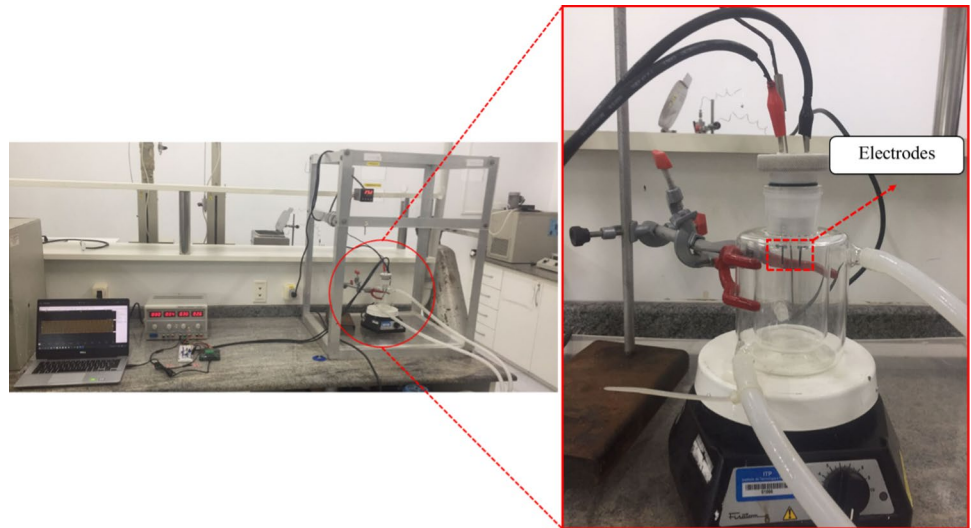
of the medium impedance, and U_{in} is the input signal from Analog Discovery 2. Both electrodes have rectangular geometry with dimensions of 21.5 mm in length $\times$ 6 mm in width (129 mm^2 area). However, only 2.0 mm in length (12 mm^2 area) was immerged in solution and used for scaling measurements as an optimization effort to fit the target area to the SEM–EDS analysis. The output signal from the current-to-potential converter was sent to the DAS to display the

acquired results (Fig. 1f) using the same Analog Discovery 2 (Fig. 1e) oscilloscope function.

2.4 Scale formation strategy

This study used two alternative techniques to generate different amounts of inorganic deposits for evaluating sensor detection. The first technique was accomplished in a single
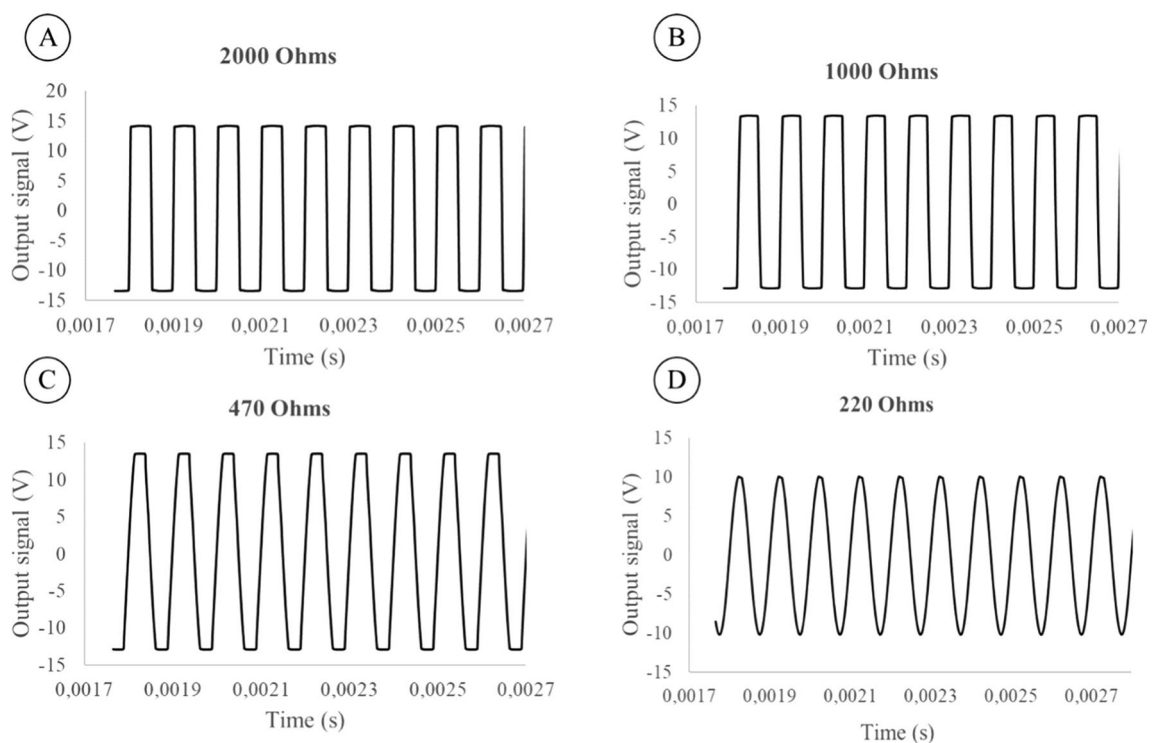

Fig. 3 Sinusoidal output signal for different gain resistor values in high-conductive saline solution at 40 °C

Fig. 4 Simulated sensor output signal, showing how the equipment behaves when different resistance levels are reached
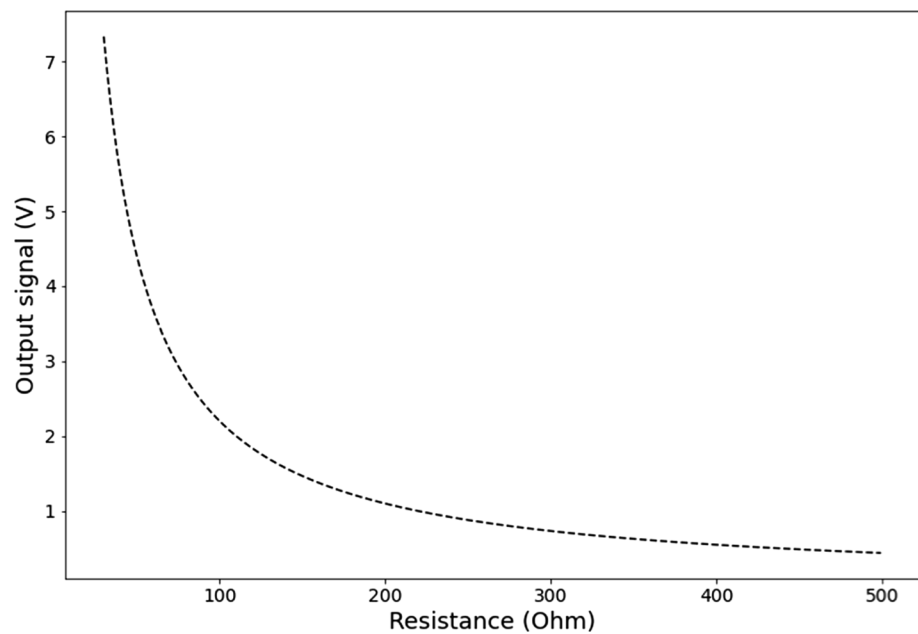

Table 2 Output signal of the system for different levels of resistance and comparison with simulated results

Resistance	Experimental output signal (V)	Simulated output signal (V)
47	9.4 ± 0.1	9.3
100	$4.4 \pm <0.1$	4.4
220	$2.0 \pm <0.1$	2.0
470	$1.0 \pm <0.1$	0.9

Table 3 Output signal measurements for each day of the experiment

Time (days)	Output signal (V)
1	24.2 ± 1.0
2	24.0 ± 0.4
3	23.1 ± 0.4
4	23.9 ± 0.2

batch, and the second employed successive batches to accelerate the deposition process.

2.4.1 Single-batch methodology

The process temperature was initially set at 40 °C using a thermostatic bath. As the temperature was established, the reactor (Fig. 2), with a full volume of 200 mL, was filled simultaneously with cation and anion solutions, ensuring a total volume of 140 mL of saline solution. An electromagnetic agitation system was added and set to 450 rpm to promote turbulence for the system. Subsequently, the electrodes were connected to the electronic part of the sensor and inserted inside the reactor with the useful electrode area totally immersed into the saline solution during the experiment.

After the insertion of electrodes into the saline solution, the measurements were initialized. This method uses an experiment lasting 4 days, with measurements accomplished each day. Measurements were collected daily to observe any signal variation attributed to electrode surface deposits.

SEM analysis was conducted at the end of the experiment to confirm the presence of scales. Such experiments were carried out in triplicate to guarantee the reproducibility of scale formation as well as the system functionality.

2.4.2 Multiple-batch methodology

For this methodology, the technique started similarly to single-batch methods, with the same experimental unit (Fig. 2), temperature adjustment, solution placement in the reactor, and sensor measurements. In addition to the first methodology, temperatures of 40 °C, 60 °C, and 80 °C were also employed in this investigation. Once the measurements were carried out, the electrodes were kept in solution for 3 h to improve scale deposition. In this study, the horizontal and vertical positions of the electrodes were used to evaluate the effect of the surface orientational position on the scale deposition. In the vertical positioning, the electrodes were placed directly on the supports for the deposition of salts and measurements. For the horizontal positioning, the electrodes were initially immersed in the bottom of the reactor and then placed on the support at the same height as the vertical positioning to perform the measurements. In this way, we ensured the
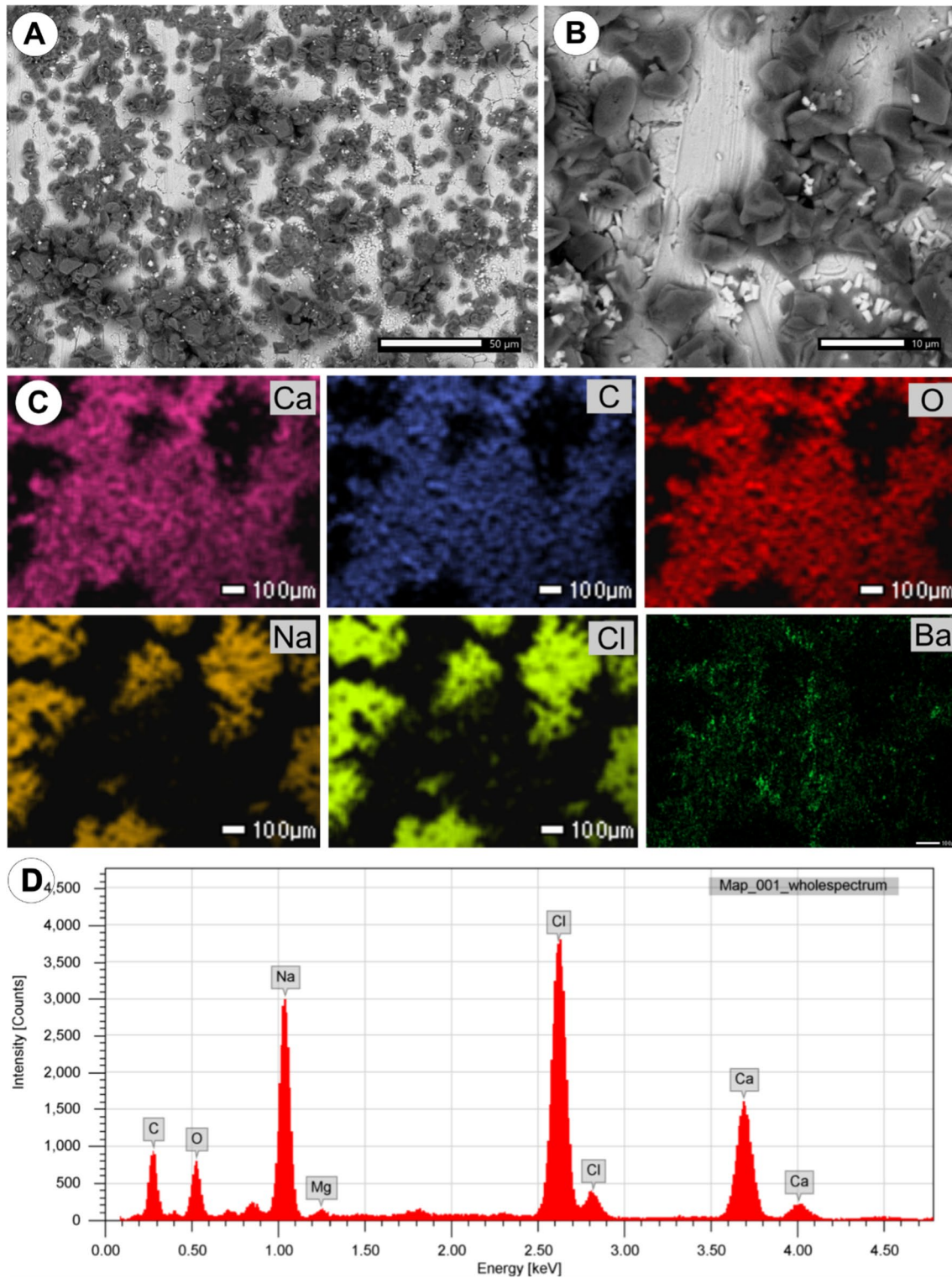
Fig. 5 Initial scale deposition behavior at 40 °C. **A–B** SEM backscattering images; **C** EDS mapping to demonstrate the spatial distribution of the inorganic deposits; **D** EDS spectrum of the scales

same height of the electrodes in all experiments. After the experimental time, the electrodes were withdrawn from the solution and placed in a hot-air circulation oven set at 90 °C for 12 h. So, the electrodes were subjected to SEM–EDS analysis on a JEOL JSM-IT200LA to analyze the deposition process. Finally, these electrodes were taken to a new saline solution for an additional deposition run. After 3 h, they were removed from the solution, dried, and analyzed by SEM, and all procedures were repeated. As the single-batch methodology, all experiments were carried out in triplicate.
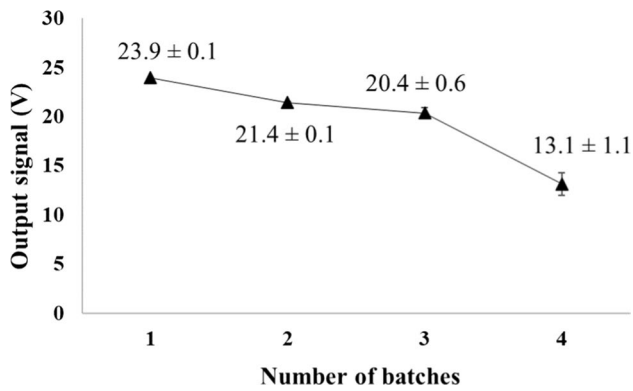
3 Results and discussion

3.1 Signal adjustment

In order to conduct scale monitoring, the first step was the signal adjustment of the system for detecting the presence of inorganic deposits by the selection of a gain resistor. This procedure was established with the saline solution used in this study as a background without the presence of Ca^{2+} to avoid the presence of inorganic deposits once $CaCO_3$ is the most suitable inorganic deposit in this solution. Given this, a propitious gain resistor for the sensor could be found (Fig. 3).
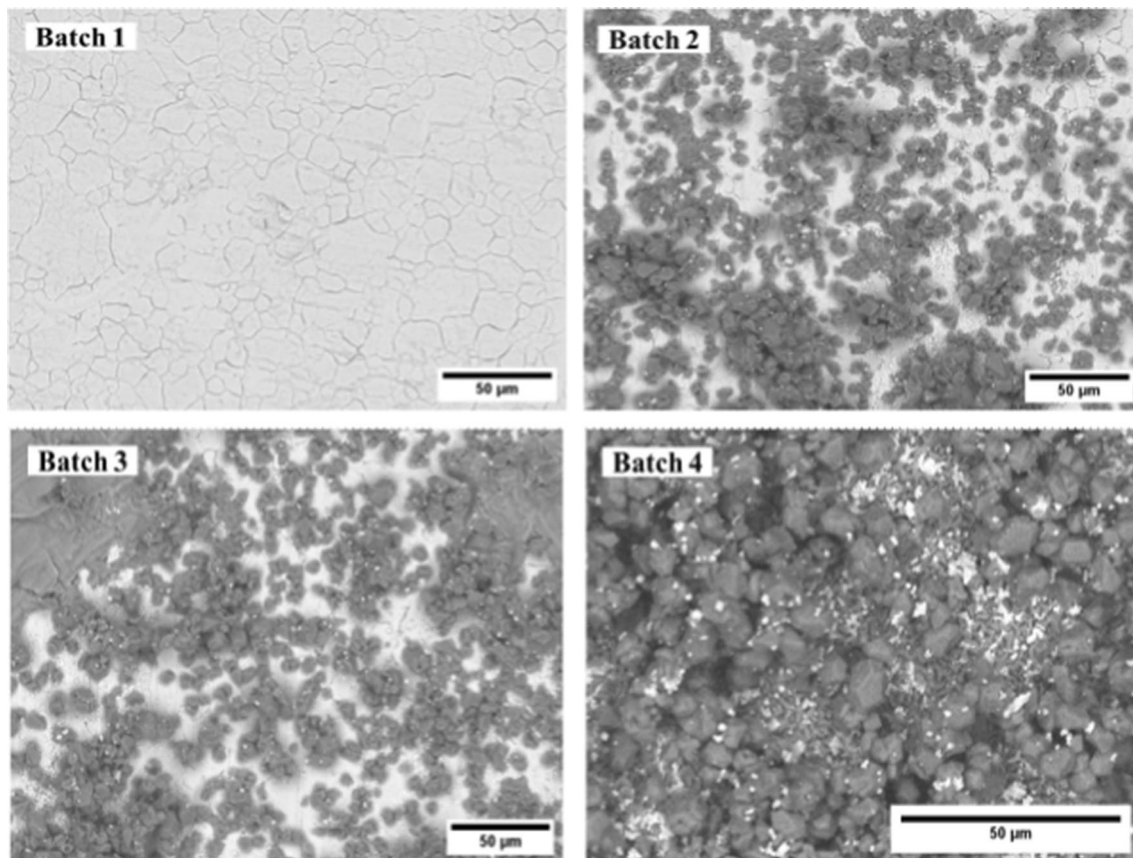

Fig. 6 Reduction of the output signal for multiple-batch methodology at 40 °C, using vertical spatial orientation

Fig. 7 SEM images of the scale formation evolution through the multiple batches at 40 °C. At *batch 1,* the electrode surface does not have scales, but salt deposition increases throughout the batches
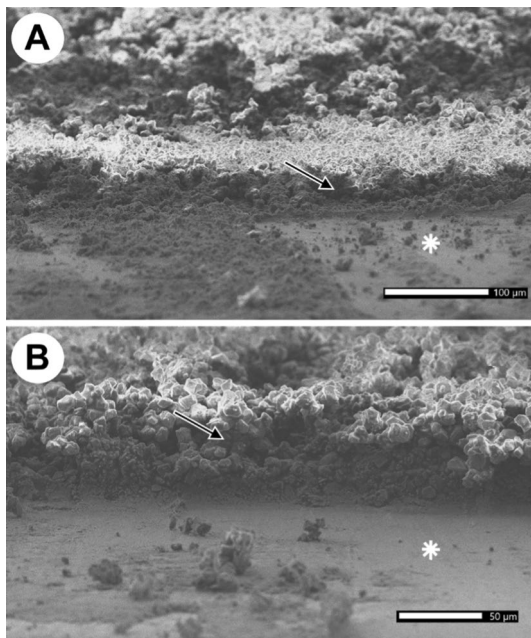
Fig. 8 SEM image cross-sectional view of the deposited scales during batch 4 at 80 ºC. **A**–**B** partial view of the salt layer height (arrow) compared to empty areas (asterisk) produced by mechanically removing scales
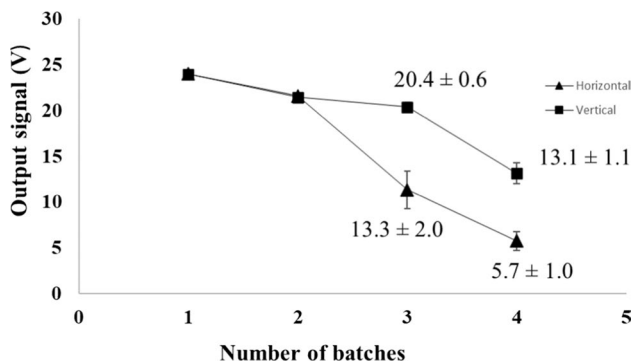

Fig. 9 Sensor output signal in each batch for the horizontal and vertical positions of the electrode

As seen in Fig. 3, the value of the gain resistor provoked different scenarios of behavior on the sensor output signal. For high values of gain resistance (Fig. 3a–c), the amplitude of signals reached conditions that go further than the limits of the operation amplifier supply, causing saturated sinusoidal signals. This behavior is attributed to the large concentration of ions in the solution, bringing low electrical resistance of the medium and, consequently, an increase in the output signal amplitude. Differently from the others, in the resistor of 220 Ohms (Fig. 3d), the characteristic of the signal indicates a more correct behavior of the system once the amplitude of the sinusoid is well defined, showing signals within the operating range of the operational amplifier.

3.2 System behavior

An important parameter for the measurements of scales is the behavior of the system for different levels of electrical resistance. In a first moment, such behavior was evaluated by simulation, using Eq. 2 for given values of resistances. Such a task was carried out by a Python script implemented *in-house* to obtain output signal amplitude with different values of R_x (simulated medium resistance) and a gain resistor value of 220 Ohms. The predictions in silico of increasing the hypothetical resistance values of the supersaturated saline solution (Fig. 4) demonstrated that sensor output values were inversely proportional to the resistance values [18]. Such behavior was also observed during experimental tests, accomplished in triplicate, using fixed resistance values (Table 2).

These results also reveal the good behavior of the system when the obtained experimental signals are compared with simulated signals generated with LTspice software. These selected resistors represent different contents of inorganic deposits on the electrodes, as seen in the below results (Fig S9 a), since the solid deposited salt matrix has poor conductivity, indicating a low output signal [17, 19]. The predicted data (Fig. 4) also indicated that the sensor signal decreases suddenly, initially revealing a region with a high sensibility to resistance. However, the mentioned sensibility considerably decreases when the resistance of the medium increases.

3.3 Scale detection

The standard value of the initial conductivity for each scaling batch was the ionic solution itself. The high availability of dissolved ionic species ensured the high conductivity of the solution [19]. There were no inorganic deposits onto the substrate for this initial step, and the sensor detected a maximum conductive signal. Therefore, as inorganic salts accumulated onto the substrate, the electrical resistance increased, registering as a decrease in the electrical output signal.

3.3.1 Single-batch scaling

The findings for the 4 days single-batch scaling did not reveal an expressive deposition of scales, as there was no substantial decrease in the voltage output signal (after a gain of signal), as seen in Table 3.
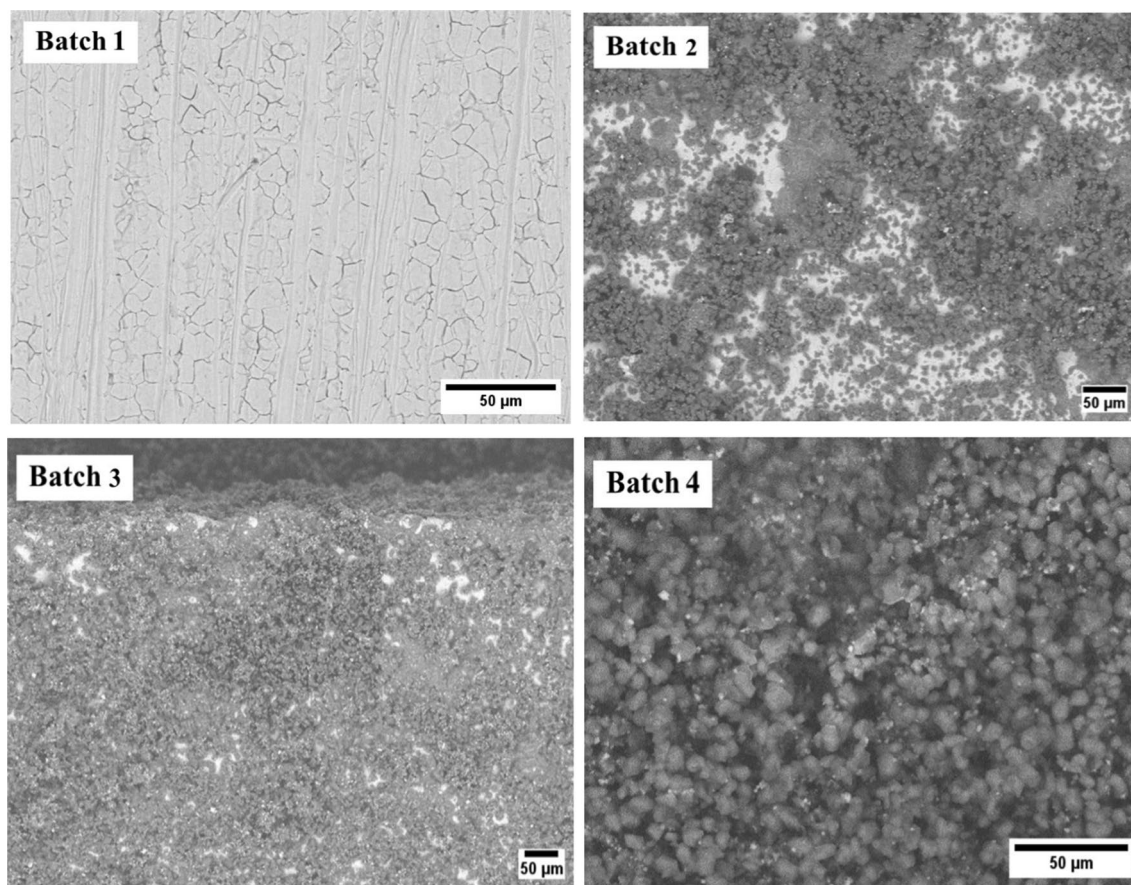
Fig. 10 Evaluation of the scaling process along the batches by SEM analysis for the horizontal surface orientation of the electrode. Observe the empty areas in batches 2 and 3 (white areas), in contrast to batch 4, which has no voids. Note the white spots in batch 4, which denotes the presence of $BaSO_4$ in combination with $CaCO_3$ crystals

An Analysis of Variance using was performed to check the influence of time on the data. By using a significance level (α) of 0.05, no statistical difference among the evaluated points was found. The sensor measurements indicated a poor salt deposition over the substrate, as confirmed through SEM images, showing salt-free areas onto the stainless-steel substrate (Fig. 5a–b). At this batch of scaling, a dominance of NaCl was observed over the other detected salts, which is concurrent with $CaCO_3$ and other salts (Fig. 5d), been such predominance confirmed by EDS mapping (Fig. 5c). Because of the sparse scaling distribution, the output signal stood high, indicating a failure of the system to detect the scale (Fig. 5).

Such an expressive number of scale-free regions is responsible for the low electrical resistance of the medium [20]. It is because a loose structure of the attached salt particle aggregates allows the electric current to pass through the saline solution and the salt-empty spaces without causing a reduction in the output signal detected by the sensor [17]. In the oilfield scenario, a high level of fouling coverage should be expected, bringing a sharp reduction in the output signal of the sensor. This behavior may be linked to the aging

Table 4 Output signal of the system for different temperatures along the batches

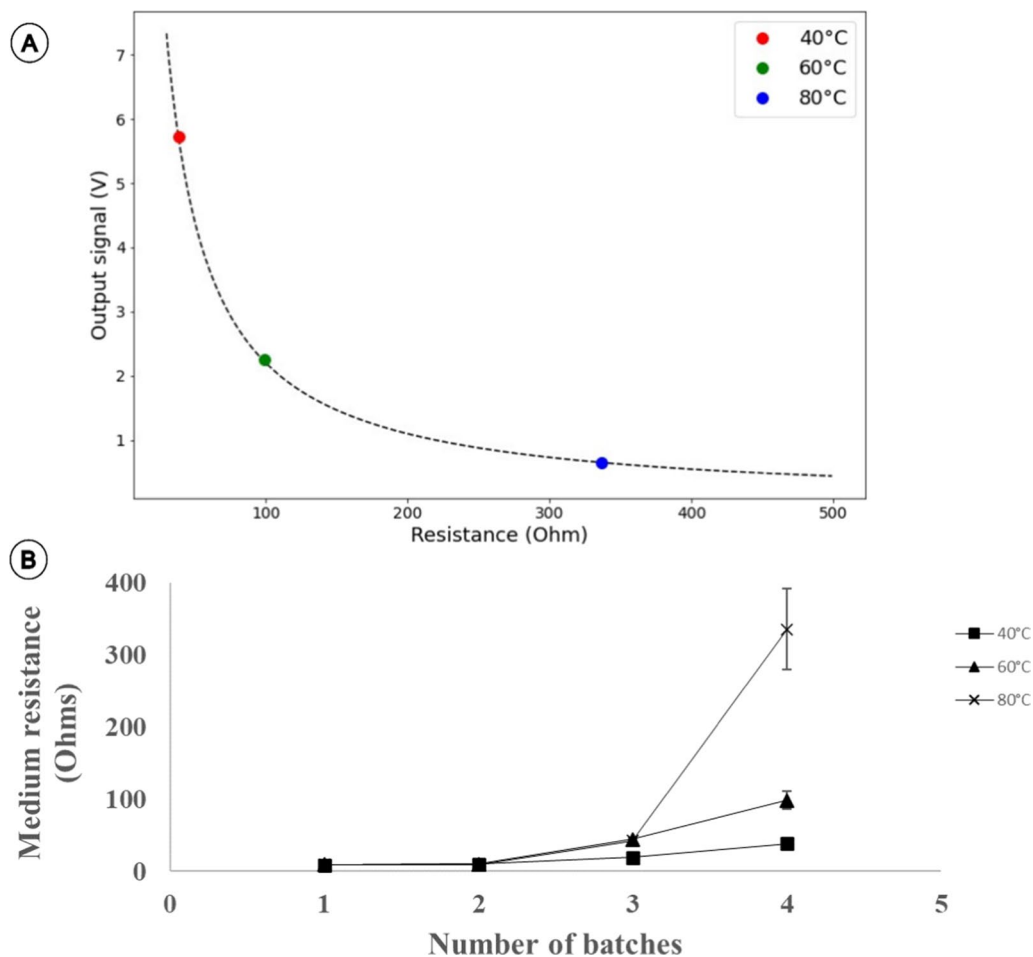| Number of batch	40 °C	60 °C	80 °C
1	23.98 ± 0.13	22.51 ± 0.15	22.36 ± 0.08
2	21.59 ± 0.08	21.86 ± 0.64	22.52 ± 0.04
3	11.31 ± 2.08	4.95 ± 0.12	5.16 ± 0.56
4	5.72 ± 1.01	2.25 ± 0.27	0.65 ± 0.11

Fig. 11 Evaluation of temperature on scale deposition. Simulated output signal of the sensor versus electrical resistance of the medium with the insertion of the result of the fourth batch sensor **A**. Electrical resistance of the medium versus the number of batches for each temperature **B**

process of fouling. Due to the drying process of nearby scale particles in the aging stage, mature mineral deposits have less water content. They may have an insulating effect on the substrate electrode due to its compactness and reduction in pore size and number [21]. It should be noted that the water content can alter the morphology and composition of the salt particles. However, as the scale crystals occur, the original crystal lattices restructure, and the crystal morphology can also change [22–24]. For this reason, the multiple-batch methodology is applied to increase the amount of deposits into the electrode.

3.3.2 Multiple-batch scaling

Multiple-batch measurements (Fig. 6) revealed a significant decrease in the output signal throughout the batches. Statistical analysis (Analysis of variance couple to t-student distribution) reinforced such difference among the batches considering a confidence level of 0.05. According to SEM observations from each batch (Fig. 7), the fouling process on the electrodes has continued progressing over the batches.

Several factors contributed to this behavior, including the re-dissolution of ionic salts and temperature fluctuations between batches. As a result of the rewetting/crystallization cycles with liquid water, new ions were reintroduced into the solution, causing them to coalesce with existing inorganic deposits [25, 26] over the electrodes, covering the empty areas (Figs. 6 and 8). Aside from crystallization, temperature also played a role in the aging process of scale formation, as mentioned before. With the increase in temperature between batches, the drying process of the electrodes resulted in high levels of supersaturation of the medium and the chemical potential of the crystals, increasing adhesion [27]. Scale adhesion can lead to heterogeneous nucleation between

Fig. 12 Evaluation of scale deposition in the fourth batch at 80 °C. ▶
SEM backscattering image **A**, EDS spectra **B–F**, and EDS elemental
mapping **G**

previously deposited scales, as seen in Fig. 8. The cross-sectional image suggests more significant nucleation of the seeds available on the substrate, resulting in the reduction of scale-free regions and, at the same time, an increase in the thickness of the fouling layer leading to a reduction of sensor signal [5, 28, 29].

3.4 Electrode spatial orientation

The position of the detection of the electrode affects the output signal. Before the electrode third batch, the orientation did not alter scale deposition since there were no substantial changes in the sensor output signal (Fig. 9). With the third batch, the decrease in output signals for the horizontal direction of the electrode became highly significant. The SEM investigation (Fig. 10) showed a significant presence of inorganic deposits in the horizontal direction. In contrast to the SEM analysis for the vertical direction (Fig. 7), the second and third horizontal batches for the horizontal orientation already indicate the production of many layers of inorganic deposits due to the coarser material. It adds to the decrease in electrode-free zones, which increases signal attenuation. This qualitative variation in the composition of inorganic deposits caused by the horizontal orientation of the electrode surface may be ascribed to the sedimentation of crystallites forming in the bulk solution and a heterogeneous crystallization process across the substrate surface based on rewetting/crystallization cycles [27, 30].

3.5 Effect of temperature

By evaluating the sensor output signal (Table 3), the temperatures of 60 °C and 80 °C showed a more conspicuous influence on the scaling process than 40 °C. This trend can be attributed to the enhanced quantity of inorganic deposits at 60 °C and 80ºC as carbonates become less soluble in solution as the temperature increases, intensifying the phenomenon of nucleation along batches [31]. Although the output signal changed significantly between 40 °C and 60 °C, the difference between 60 °C and 80 °C was less noticeable. According to the observed data (Table 4), the difference in the signal response for the last two temperatures was more evident in the fourth batch.

This tiny change in the sensor output signal can be attributed to its behavior with medium resistance. When the findings of the fourth batch of sensor data were fitted into the
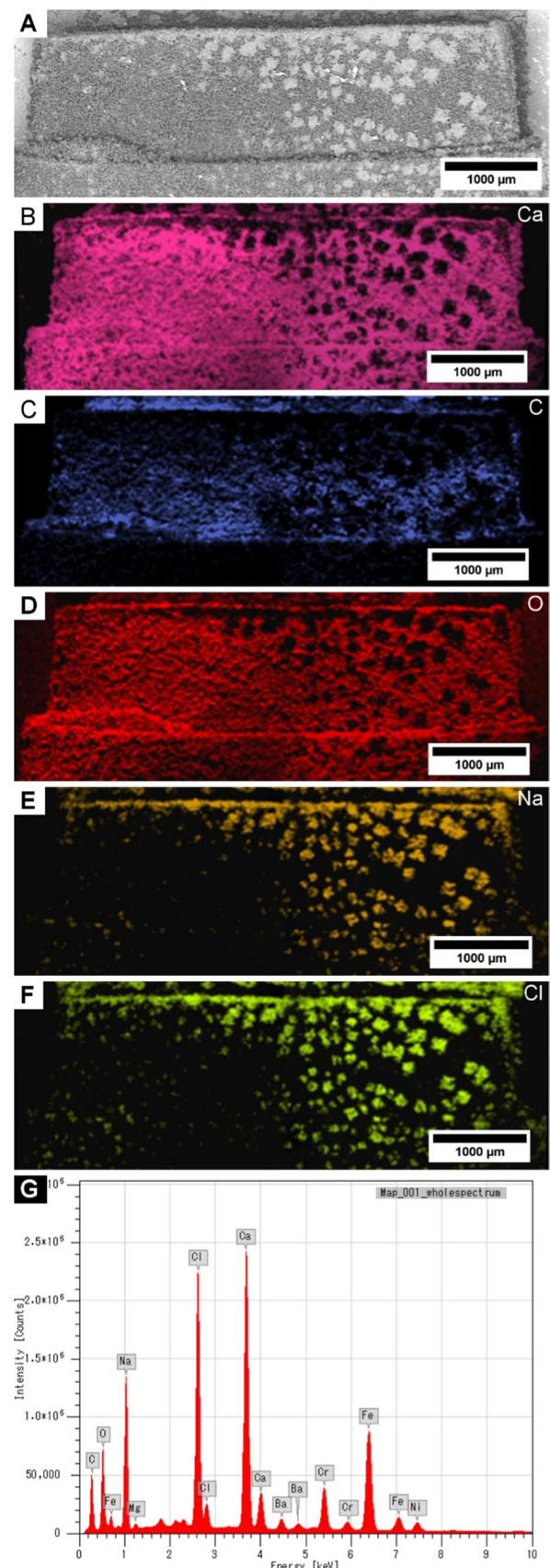
sensitivity curve (Fig. 11a), it was evident that the locations for high temperatures (60 °C and 80 °C) were in the low sensitivity zone of the sensor, necessitating more effort to analyze the signal fluctuation. This difference is magnified when the output signal is modified by the predicted electrical resistance of each batch of medium (Fig. 11b). In the fourth batch, the results are very different depending on the temperature, showing how temperature can influence the thermodynamic equilibrium of the ionic compounds.

The spatial distribution of the minerals deposited on the electrodes in batch 4 (Fig. 12c) is formed mainly by $CaCO_3$ (with presence in almost the entire electrode surface), followed by NaCl zones and low Ba content, indicating the formation of $BaSO_4$. Intensity peaks of the EDS spectrum (Fig. 12b) confirm a significant predominance of calcium, reinforcing the increase in $CaCO_3$ due to the temperature effect. In terms of found elements, it agrees with previous results (Fig. 5) in this work.

4 Conclusions

A new measurement technique for inorganic scale detection in high ionic solution concentrations was developed. The electrical measurement system proved to be effective in detecting fouling on the surface of stainless-steel electrodes. The amount of inorganic deposition on the surface of the stainless-steel electrodes was indicated by the signal intensities of the sensor system. The evolution of the fouling process over the multiple-batch methodology was validated using SEM combined with EDS chemical spatial distribution. The detection of the fourth batch of scale deposition at higher temperatures demonstrated improved results. $CaCO_3$, NaCl, and $BaSO_4$ were the most common crystals in the scale composition, which coincides with supersaturated salt solution ions. The results presented in this work can be helpful as a new sensor capable of monitoring different types of fouling at high ionic concentration levels while evaluating physical parameters that influence scale formation.

Data availability Data sharing does not apply to this article as no datasets were generated or analyzed during the current study.

Declarations

Conflict of interest The authors declare that they have no potential conflicts of interest.

Human or animal rights Not applicable to this study.

Informed consent For this type of analysis, formal consent is not needed.

References

1. Qazvini S, Golkari A, Azdarpour A, Santos RM, Safavi MS, Norouzpour M (2021) Experimental and modelling approach to investigate the mechanisms of formation damage due to calcium carbonate precipitation in carbonate reservoirs. J Pet Sci Eng 205:108801. https://doi.org/10.1016/j.petrol.2021.108801
2. World Bank (2022) Commodity Markets Outlook: The Impact of the War in Ukraine on Commodity Markets, April 2022. World Bank, Washington, DC. License: Creative Commons Attribution CC BY 3.0 IGO.
3. Valbuena G (2010) Challenges of deepwater development. Offshore Mag.
4. Bader MSH (2007) Sulfate removal technologies for oil fields seawater injection operations. J Pet Sci Eng 55:93–110. https://doi.org/10.1016/j.petrol.2006.04.010
5. Liu J, Zhou F, Dai Q, Gao H (2021) Effect of Ca^{2+}, Mg^{2+}, Ba^{2+} and Sr^{2+} cations on calcium carbonate scaling formation in oil-gas well: based on density functional theory study and molecular dynamics simulation. J Cryst Growth 563:126089. https://doi.org/10.1016/j.jcrysgro.2021.126089
6. Feng C, Zhang P (2022) Control of composite oilfield scales and deposits. Water-Form Depos. https://doi.org/10.1016/j.jcrysgro.2018.07.037
7. Kamal MS, Hussein I, Mahmoud M, Sultan AS, Saad MAS (2018) Oilfield scale formation and chemical removal: a review. J Pet Sci Eng 171:127–139. https://doi.org/10.1016/j.petrol.2018.07.037
8. Kelland MA (2014) Production chemicals for the oil and gas industry, 2nd edn. CRC Press/Taylor & Francis, Boca Raton, FL
9. Thant MMM, Sallehud-Din MTM, Hewitt GFF, Hale CPP, Quarini GLL (2011) Mitigating flow assurance challenges in deepwater fields using active heating methods. OnePetro. https://doi.org/10.2118/140997-MS
10. Rostron P (2018) Critical review of pipeline scale measurement technologies. Indian J Sci Technol 11:1–18. https://doi.org/10.17485/ijst/2018/v11i17/121459
11. Zuo Z, Yang W, Zhang K, Chen Y, Li M, Zuo Y, Yin X, Liu Y (2020) Effect of scale inhibitors on the structure and morphology of $CaCO_3$ crystal electrochemically deposited on TA1 alloy. J Colloid Interface Sci 562:558–566. https://doi.org/10.1016/j.jcis.2019.11.078
12. Feasey ND, Freiter E, Jordan MM, Wintle R (2000) Field Experiences with a Novel Near Real Time Monitor for Scale Deposition in Oilfield Systems. OnePetro
13. Emmons DH, Graham GC, Holt SP, Jordan MM, Locardel LP, Locardel B (1999) On-Site. OnePetro, Near-Real-Time Monitoring of Scale Deposition. https://doi.org/10.2118/56776-MS
14. de Souza AVA, Rosário F, Cajaiba J (2019) Evaluation of calcium carbonate inhibitors using sintered metal filter in a pressurized dynamic system. Materials 12:1849. https://doi.org/10.3390/ma12111849
15. Christidis K, Gunarathne GP, Peteineri K (2013) Intelligent instrumentation for identification of scales in petroleum pipelines *in situ*. Trans Inst Meas Control 35:457–463. https://doi.org/10.1177/0142331212453598
16. Salgado CM, Salgado WL, de Freitas Dam RS, Conti CC (2021) Calculation of scales in oil pipeline using gamma-ray scattering

and artificial intelligence. Measurement 179:109455. https://doi.org/10.1016/j.measurement.2021.109455

17. Wong P-Z (1999) 4. Conductivity, Permeability, and Electrokinetics. In: Wong P (ed) Experimental Methods in the Physical Sciences. Academic Press. https://doi.org/10.1016/S0076-695X(08)60415-9

18. Frias MAR, Yang W, (2016) Electrical resistance tomography with voltage excitation, I: 2016 IEEE International Instrumentation and Measurement Technology Conference Proceedings, https://doi.org/10.1109/I2MTC.2016.7520444.

19. Haddad PR, Jackson PE (1990) Chapter 9 Conductivity Detection. In: Ion chromatography: principles and applications. Elsevier, Kensington, https://doi.org/10.1016/S0301-4770(08)61141-0

20. Edvardsen L, Gawel K, Wenner S, Gawel B, Torsaeter M (2020) Electrochemical enhancement and inhibition of calcium carbonate deposition. J Environ Chem Eng 8:104239. https://doi.org/10.1016/j.jece.2020.104239

21. Dervos CT, Mergos JA, Iosifides AA (2005) Characterization of insulating particles by dielectric spectroscopy: case study for $CaCO_3$ powders. Mater Lett 59:2842–2849. https://doi.org/10.1016/j.matlet.2005.03.066

22. Schmidt MP, Ilott AJ, Phillips BL, Reeder RJ (2014) Structural changes upon dehydration of amorphous calcium carbonate. Cryst Growth Des 14:938–951. https://doi.org/10.1021/cg401073n

23. Ihli J, Wong WC, Noel EH, Kim Y, Kulak AN, Christenson HK, Duer MJ, Meldrum FC (2014) Dehydration and crystallization of amorphous calcium carbonate in solution and in air. Nat Commun 5:3169. https://doi.org/10.1038/ncomms4169

24. Han Y, Zhang C, Wu L, Zhang Q, Zhu L, Zhao R (2018) Influence of alternating electromagnetic field and ultrasonic on calcium carbonate crystallization in the presence of magnesium ions. J Cryst Growth 499:67–76. https://doi.org/10.1016/j.jcrysgro.2018.07.037

25. Desarnaud J, Bertrand F, Shahidzadeh-Bonn N (2013) Impact of the kinetics of salt crystallization on stone damage during rewetting/drying and humidity cycling. J Appl Mech 80:020911–020998. https://doi.org/10.1115/1.4007924

26. Shahidzadeh-Bonn N, Desarnaud J, Bertrand F, Chateau X, Bonn D (2010) Damage in porous media due to salt crystallization. Phys Rev E 81:066110. https://doi.org/10.1103/PhysRevE.81.066110

27. Steiger M (2005) Crystal growth in porous materials—I: the crystallization pressure of large crystals. J Cryst Growth 282:455–469. https://doi.org/10.1016/j.jcrysgro.2005.05.007

28. MacAdam J, Parsons SA (2004) Calcium carbonate scale formation and control. Rev Environ Sci Biotechnol 3:159–169

29. Zhao J, Wang M, Lababidi HMS, Al-Adwani H, Gleason KK (2018) A review of heterogeneous nucleation of calcium carbonate and control strategies for scale formation in multi-stage flash (MSF) desalination plants. Desalination 442:75–88. https://doi.org/10.1016/j.desal.2018.05.008

30. Wang H, Alfredsson V, Tropsch J, Ettl R, Nylander T (2013) Formation of $CaCO_3$ deposits on hard surfaces—effect of bulk solution conditions and surface properties. ACS Appl Mater Interfaces 5:4035–4045. https://doi.org/10.1021/am401348v

31. Serpa FS, Silva GM, Freitas LFL, Filho EBM, Nascimento JF, Pereira LS, Salazar-Banda GR, Borges GR, Dariva C, Franceschi E (2022) An experimental study of calcium carbonate precipitation with hydrate inhibitor in MEG recovery unit. Upstream Oil Gas Technol 8:100061. https://doi.org/10.1016/j.upstre.2021.100061